Indian J. Met. Hydrol. Geophys. (1975), 26, 3, 399-404

551·558·21(54) "322·1"

Vertical velocity patterns over India and neighbourhood during break monsoon and active monsoon periods

R. K. DATTA and T. K. MUKERJI

Meteorological Office, New Delhi

ABSTRACT. Vertical velocity patterns at different levels of the atmosphere, over India and neighbouring areas have been obtained for a situation each of active and break monsoon. A five-layer quasi-geostrophic model has been developed for the above computations. These vertical velocity patterns are discussed to bring out their salient features and their differences. A model for the vertical velocity field for active/break monsoon has also been proposed.

1. Introduction

Southwest monsoon over the Indian region is well known for its pulsating nature. There are periods of heavy rain caused by depressions moving northwestward along the axis of the monsoon trough. There are also periods of lull in the rainfall over most parts of the country, better known as 'break' in the monsoon. These breaks normally last for a short period, but in some cases have continued for 21 days. These long periods of deficient rainfall lead to serious drought conditions in the country with far reaching repercussions on Indian agriculture and economy. Thus break monsoon periods are of importance and interest to meteorologists and agriculturists alike.

In this paper we have studied one break monsoon and one active monsoon situation, by computing the vertical velocity ω fields at different levels. The salient features of these ω fields are presented here. The ω fields for the active monsoon period have also been compared to those obtained by Das (1962) using a ten-layer quasi-geostrophic model. Certain interesting aspects of these ω patterns over the Arabian Sea are also discussed.

2. Method for computation of vertical velocity

Quasi-geostrophic ω equation (QGWE) and its sclution

Vertical velocity ω can be obtained by solving the QGWE under suitable constraints by using a ten-layer model (Das *et al.* 1970). A four-layer model was discussed by Mukerji and Datta (1972), where the QGWE was solved for adiabatic conditions. Diagnostic and prognostic ω values have been obtained by a diabatic four layer model also, where the effect of the release of latent heat radiation and ground contours are included (Mukerji and Datta 1973). In the present study, the same scheme has been used, with some modifications. Thus, the four-layer model has been converted into a five-layer one by extending the upper most level to the top of the atmosphere. The vertical grid is shown in Fig. 1. Horizontal grid dimension is 381 km, true at Lat. 22½° N of Mercator projection chart. The mesh comprises 31 grid points along the abscissa and 16 in the ordinate, making a total of 496 nodal points.

The horizontal boundary condition assumes ω to be zero at the boundaries. The vertical boundary condition takes ω as zero at the top of the atmosphere. At the bottom (1000 mb level) ω is computed with the help of ground contour values.

Under the above boundary conditions it is possible to solve the QGWE, given below, after converting it into finite difference form.

$$\sigma_k \nabla^2\omega_k - \frac{f^2 d^2}{gm^2(\nabla p)^2}(\omega_{k-1} - 2\omega_k + \omega_{k+1}) = \frac{g}{8fd^2\triangle p}\nabla^2 m^2 \mathbf{J}(Z_{k+\frac{1}{2}} + Z_{k-\frac{1}{2}}, Z_{k+\frac{1}{2}} - Z_{k-\frac{1}{2}}) - \frac{1}{4\triangle p}\left[\mathbf{J}(Z_{k+}, \zeta_{k+\frac{1}{2}} + f) - \mathbf{J}(Z_{k-\frac{1}{2}}, \zeta_{k-\frac{1}{2}} + f)\right] + Q \quad (1)$$

The symbols have their standard meaning. The details of the mathematical manipulations have been published elsewhere (Mukerji and Datta 1973).

The effect of surface drag was not taken into account in earlier models and the same has been included in this study by utilising the formula of Haltiner (1971) :

$$\omega_{\text{friction}} = \frac{g}{f}\left[\frac{\partial}{\partial y}(\rho_0 C_D u_0 v_0) - \frac{\partial}{\partial x}(\rho_0 C_D u_0 v_0)\right] \quad (2)$$

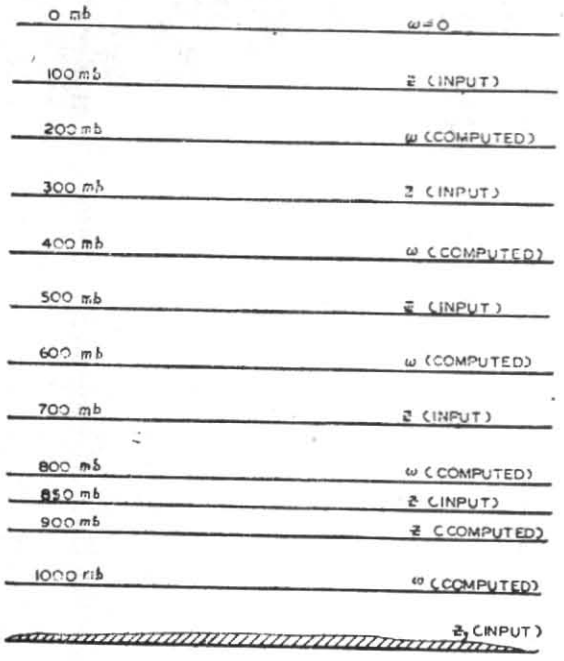

Fig. 1 Vertical grid for ω computation. Z =contour values, ω =vertical velocities and Z_g =ground contours

The drag coefficient, C_D, is supplied at all the grid points over the area of integration.

Finite difference approximation

All finite difference approximations were of the centred difference type. Thus, for any quantity A,

$$A_x = (A_{i,j+1} - A_{i,j-1}) / 2d$$

$$A_y = (A_{i+1,j} - A_{i-1,j}) / 2d$$

$$\nabla^2 A = (A_{i+1,j} + A_{i,i-1} + A_{i-1,j} + A_{i,j+1} - 4A_{i,j}) / 4d^2$$

$$\mathbf{J}(A,\zeta) = [(A_{i+1,j} - A_{i-1,j})(\zeta_{i,j+1} - \zeta_{i,j-1}) - (A_{i,j+1} - A_{i,j-1})(\zeta_{i+1,j} - \zeta_{i-1,j})] / 4d^2 \quad (3)$$

where d includes the map factor. More elaborate finite difference expressions could be used. However the above simple scheme gives results for diagnostic cases with almost comparable accuracy as with more refined schemes (Hawkins 1972). As such, these simple expressions for Laplacian and Jacobian were used.

Use of smoother

To reduce the error introduced by the finite difference approximation, the following mild smoother was applied on the initial data, before the processing was started :

$$A_{i,j} = [A_{i-1,j} + A_{i+1,j} + A_{i,j-1} + A_{i,j+1} + 4A_{i,j}] / 8 \quad (4)$$

This helps to remove inaccuracies in the form of small waves, which could otherwise vitiate the solution of the ω equation.

Relaxation procedure

The quasi-geostrophi ω equation is solved by an inerative procedure known as Extrapolated Liebmann Method. In this process, a guess value is supplied for ω in Eq. (1) and a residual RES is obtained, since this guess does not satisfy that equation. Now we put $\omega^{N+1}_{i,j,k} = \omega^{N}_{i,j,k} + \alpha \mathrm{RES}^{N}_{i,j,k}$ where α is the over relaxation factor and N, the number of iterations. The new value of $\omega_{i,j,k}$, that is $\omega^{N+1}_{i,j,k}$ is used in the calculation of other ω values in the same iteration. The iterations are carried out over all the grid points of the model till RES is reduced to zero or to a value less than a pre-set tolerance limit. To save computer time it is necessary to choose a suitable value of α, which determines the rate of convergence of the iteration. For this study we have chosen α as 0.30 and with this value the number of iterations was kept below 20 in most cases.

Tolerance for relaxation

We have chosen the tolerance for residual in case of ω as 10^{-3} cm/sec. Since, the ω values computed are of the order of 1 cm or more, this tolerance limit is considered to be reasonable. Thus the ω values presented in this study are accurate to 0.001 cm/sec only.

3. Data utilised

During 1966, the period between 23 & 27 August had very little rainfall and had been chosen for study as an example of break monsoon. The same period in 1967 exhibited normal monsoon characteristics and has been studied to depict active monsoon situation. The rainfall charts for two days each of these periods shown in Figs. 2 & 3 respectively, clearly bring out the break-monsoon and active-monsoon nature. Constant pressure charts of all the levels were analysed for the above periods with special attention to their vertical consistancy and day-to-day continuity. This is found to be particularly important, as any error in the input data of one level, gets transmitted to the other levels during the process of three dimensional relaxation which is employed in the solution of the quasi-geostrophic ω equation.

Grid point values of contours at 100, 300, 500 and 700 mb were interpolated from the synoptic charts. The same for 900-mb level were computed

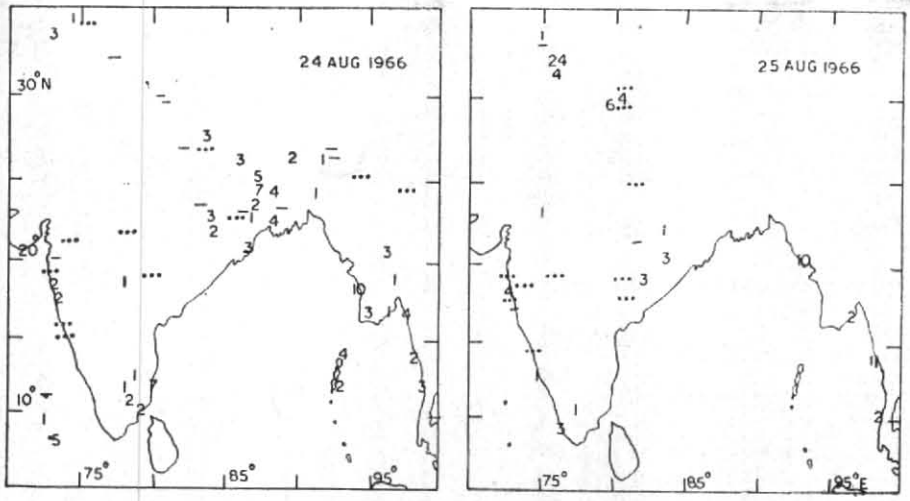

(a) 24 Aug 1966 (b) 25 Aug 1966

Fig. 2. 24-hr rainfall in break monsoon

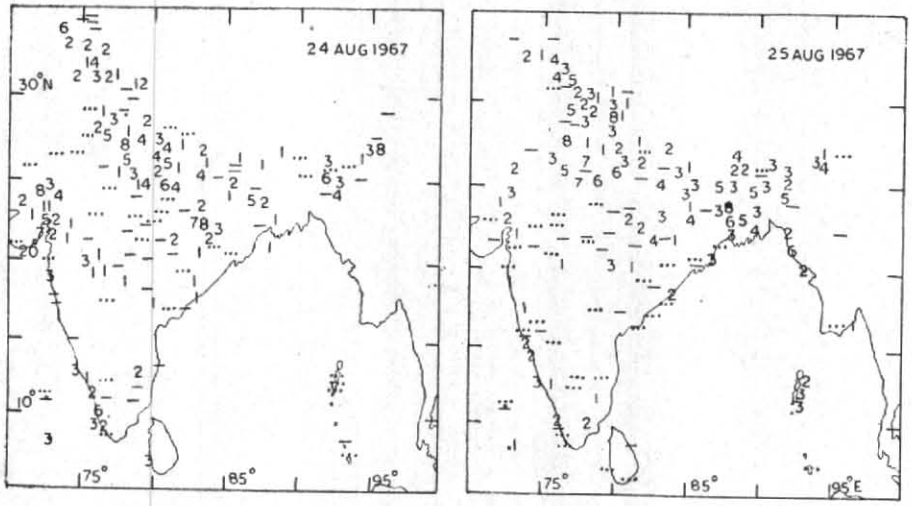

(a) 24 Aug 1967 (b) 25 Aug 1967

Fig. 3. 24-hr rainfall in active monsoon

from those of 850-mb level by the subtraction of 500 gpm uniformly. This is a very approximate mode of obtaining the 900 mb grid point values; but experience shows that it leads to acceptable results. Other relations exist for doing the same, and they connect the 900 mb height to those of 850 and 700-mb levels. Since in the 850 and 700 mb synoptic charts, the data over the Himalayas are not available, the grid point values there are hypothetical. It was therefore considered appropriate to compute the 900 mb values from only one set of hypothetical values (those of 850 mb) instead of two such sets.

4. Discussion of results

The vertical velocity patterns at 200, 400, 600, 800 and 1000-mb levels have been obtained for five-day periods of active monsoon and break monsoon periods mentioned earlier. In addition, the contour values were averaged at each grid point for the respective five day periods, to obtain the average ω patterns. An examination of these ω patterns indicate that the average patterns are good reflections of the individual patterns, and as such, we discuss below the average ω patterns only.

4.1. *Average active monsoon ω-pattern*

Fig. 4 shows the average vertical velocity features, for active monsoon period between 23 and 27 August 1967. Discussion which follows will be confined to India and its neighbouring areas only. Upward and downward vertical velocity areas are indicated by arrow heads.

At 1000-mb level, marked ascent can be seen all along the west coast and descent of similar magnitude along the east coast of India. The effect of the Western Ghats in producing upward movement

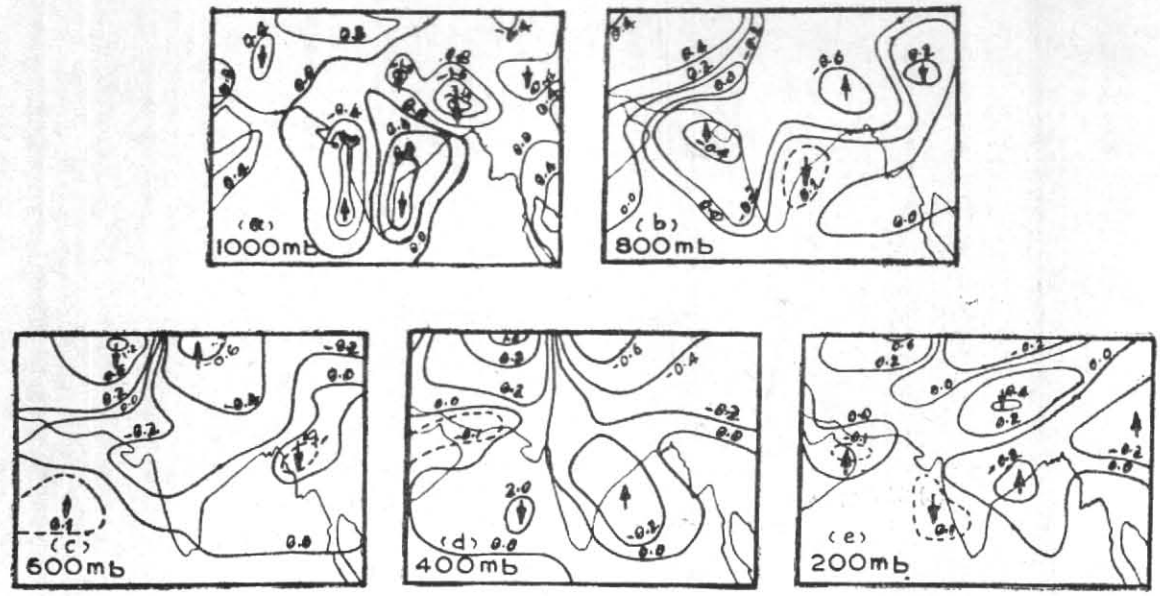

Fig. 4. Vertical motion ω field during active monsoon situation between 23 and 27 August 1967

is thus clearly brought out. It may be noticed that the upward movement starts about 400 km west of the Ghats. This feature was inferred from the cloud observation during IIOE (Das 1968 and Desai 1967) also, but there the upward motion was observed at a distance of 200 km only.

Areas of ascent are also seen over China, north east India and Russian area, extending from Lat. 21.8° N, Long. 115°E to Lat. 37.7°N, Long. 76°E. The portion of this upward ω field over north India seems to closely follow the axis of the monsoon trough.

Subsidence is seen over Indo-China, parts of China and over Russian area close to Tashkent. Over most of the Arabian Sea and Bay of Bengal ω field is rather weak.

A comparison with the ω charts obtained by Das (1962) based on the ten-layer, quasigeostrophic adiabatic model is of interest. Since he has not given the 1000 mb ω pattern, we compare his 900 mb pattern with the present 1000 mb one. It is seen that the two agree well over the Western Ghats and northeast India. Over northwest India, however, Das gets an intense area of subsidence. We however find this area of descent shifted further to the north. This can probably be attributed to the fact that Das's charts relate to normal July situation and ours to an active monsoon situation in August. In this context, the difference of 100 mb between the two charts under comparison, may have also some effect.

The 800 mb ω patterns show some difference from those at 1000 mb. Thus, the intensity of subsidence along the east coast of India becomes less and the centre of upward ω along west coast of India shifts to the north. The axis of the area of up current over northwest India becomes more northerly in orientation. Over Indo-China, area of updraft has replaced the area of downdraft seen at 1000-mb level. Over the Arabian Sea, an extension of the downward ω area seems to be taking place from the African area. Position of the subsidence area near Tashkent is maintained at this level also.

At 600-mb level, the ω pattern changes over the west coast of India, in that it becomes less intense, although it retains its upward movement. The whole upward ω area however has shifted northwards, with the result that over the Arabian Sea an area of subsidence appears. Over the east coast a feeble area of ascent has come in and the area of subsidence has been shifted to Bangladesh and adjoining areas. Thus a spectacular feature seems to be the occurrence of a reversal of ω pattern at 600 mb over India and neighbourhood, south of Lat. 20°N.

At 400-mb level, the process of reversal of the ω fields south of Lat. 20°N has been completed. An area of ascent over east coast of India is very prominent and area of descent now covers the whole of Arabian Sea. African and Somalia areas now have upward vertical velocity and the same have become insignificant over Indo-China. The area of descent over Russian Turkistan near Tashkent continues to be intense and unchanged in position.

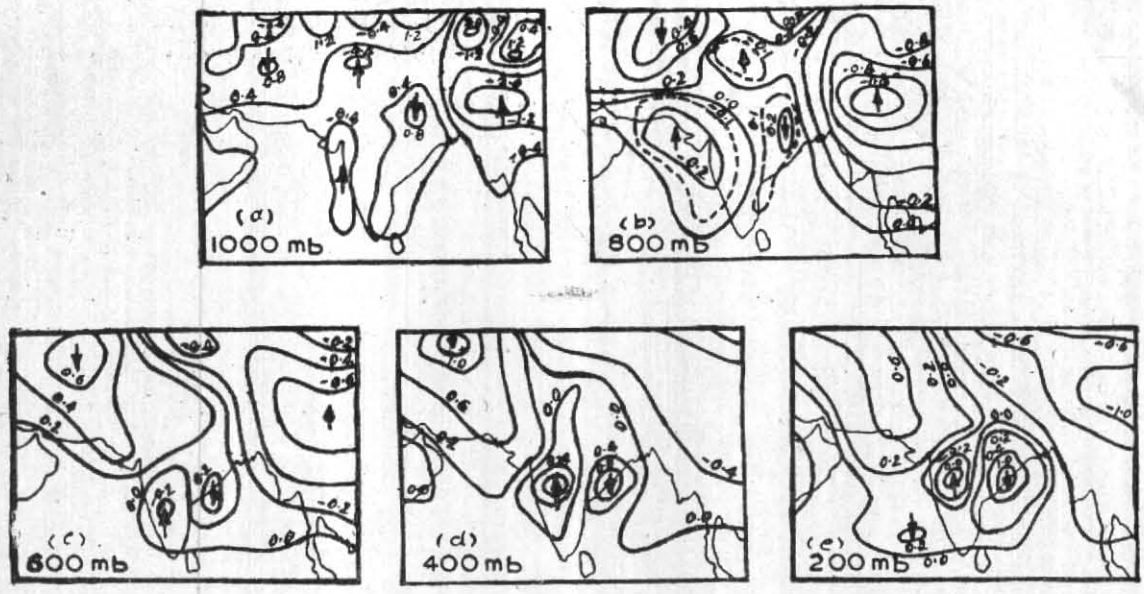

Fig. 5. Vertical motion (ω field) during break monsoon situation during 23 and 27 August 1966

A comparison with Das's (1962) chart for 500-mb level with our 400-mb chart bring out the fact that they are quite similar although the intensities of the ascent and descent areas differ in magnitude. The main difference is seen over the east Arabian Sea where he has obtained feeble upward movement, whereas we have got downward motion.

At 200-mb level, the pattern seen at 400 mb more or less persists. However, over the Himalayas an area of descent is observed. This feature does not agree with the results of Das, although other aspects of ω field at this level correspond well with his findings. Saha (1968) has also given the vertical motion field for active monsoon case of July 1963. His scheme is based on calculating ω by stepwise integration of divergence field. As has been indicated by the author himself, kinematic method has the problem of rapid increase of ω with height. Keeping this aspect in view, it may be noticed that, whereas Saha gets a single rising cell over the Indian area upto 500-mb and subsidence over sea areas on both sides of it, we get multicellular structure as discussed above. Lack of detail in his results may be ascribed to the different technique of computation over a grid of 5° length.

4.2. *Average break monsoon ω patterns*

There does not seem to be any study made so far about vertical velocity patterns over India during break monsoon period. Our study relates to break monsoon period between 23 and 27 August 1966. The ω profiles based on the five-day mean are shown in Fig. 5.

At 1000-mb level, areas of ascent over the west coast of India and areas of descent over the east coast of the country can still be seen; but compared to the active monsoon case, they are both less intense. Over northeast India, areas of ascent seen on the active monsoon case have been replaced by an area of descent. North of Jammu & Kashmir, the pattern is similar in both cases. Over China, an area of upward motion is seen during break monsoon period and very feeble upward velocity is observed over Indo-China.

ω pattern remains unchanged from the active monsoon case over the African area during break monsoon.

At 800-mb level, the ω pattern over most of India is similar to those of active monsoon case. However, over China, an area of ascent is very prominent. Over parts of north India an area of updraft is seen, but it is covered on both sides by areas of downdraft. Over northeast India also a small area of downdraft is seen during break monsoon but not during active monsoon.

At 600-mb level, the ω pattern over India is similar to that at 800-mb level. Over the Arabian Sea ω is negligible, whereas it is downwards, in active monsoon. 400 mb charts continue to depict the same features over south India as at 800 and 600-mb level and continues upwards even upto 200-mb level. At 200 mb, however, descent becomes more prominent over the Arabian Sea.

4.3. *Comparison of two ω patterns*

One salient feature which emerges from a comparison of the active monsoon with break mon-

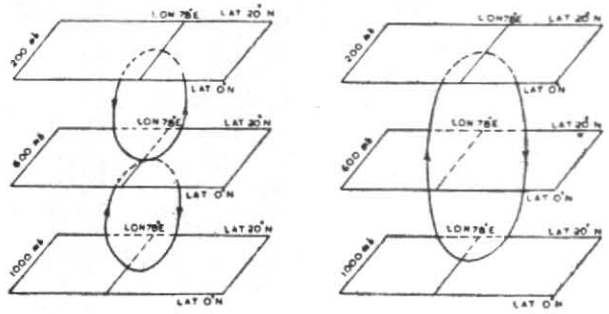

(a) Active monsoon (b) Break monsoon

Fig. 6. ω structure profile

soon ω charts, is shown in Fig. 6. These depict vertical velocity pattern with height. It becomes clear that during active monsoon, vertical velocity south of Lat. 20°N undergoes a reversal, from upward to downward, at about 600-mb level, but during break monsoon this reversal is absent.

In this context, a comparison of the model for active monsoon period given herein, to that given by Koteswaram (1958) is of interest. In the latter model a single vertical cell is seen, extending upto the tropical tropopause, between equator and Lat. 28°N . In our model, this single cell is broken up into two, as discussed earlier. In a study for normal July charts (to be reported separately) we find Koteswaram's model is justified by our computations of ω. It may thus be inferred that, when only active monsoon cases are considered the cellular structure is broken at 600-mb level. However when an average is made for both active and break monsoon cases, only a single vertical cell is observed.

5. Concluding remarks

In the above discussions we have tried to bring out the prominent aspects of the vertical velocity patterns during active and break monsoon periods over India and the difference between the two. A model for the vertical velocity field has also been suggested for the area south of Lat. 20°N.

Although these results are based on five-day average of only two situations and as such, should be considered as tentative only, these do seem to confirm the view of Ramage (1965), that subsidence not only dominates Pakistan, Arabia and Somalia but the central and western Arabian Sea also, during normal monsoon period. During break monsoon, our study indicates subsidence to be very little over Africa, Arabia and Arabian Sea areas.

Acknowledgements

We are grateful to Dr. P.S. Pant, Director, Northern Hemisphere Analysis Centre for guidance and many helpful suggestion. We also thank Shri Roy Chowdhry for the photographs, Shri Hari Krishan for diagrams and Shri J. K. Wahi for the preparation of manuscript.

REFERENCES

Das, P. K.	1962	*Tellus*, **14**, pp, 212-220.
	1968	*The Monsoons*, National Book Trust, NewDelhi, pp. 65-68
Das, P. K., Datta, R. K. and Chhabra, B. M.	1971	*Indian J. Met. Geophys.*, **22** pp. 331-333.
Desai, B. N.	1967	*J. atoms. Sci.*, **24**, pp. 216.
Haltiner, G. J.	1971	*Numerical Weather Prediction*, John Wiley & Sons, Inc., New York, pp. 151-153.
Hawkins, H. F.	1972	NOAA Tech. Memorandum ERL NHRL- 08.
Koteswaram, P.	1958	*Monsoons of the World* , India Met. Dep.
Mukerji, T. K. and Datta, R. K.	1973	*Indian J. Met. Geophys.*, **24**, pp 93-100.
	1973	*India Met. Dep. Sci. Rep.* No. 191.
Ramage, C. S.	1965	*Proc. Symp. Met. Results of IIOE.*
Saha, K. R.	1968	*Tellus*, **20**, pp. 601-620.